ELSEVIER

Physica A 315 (2002) 330–341

PHYSICA A

www.elsevier.com/locate/physa

Responses of the complex Ginzburg–Landau equation under harmonic forcing

Jeenu Kim[a], Jysoo Lee[b,*], Byungnam Kahng[a]

[a] *School of Physics and Center for Theoretical Physics, Seoul National University, Seoul 151-742, South Korea*

[b] *Supercomputing Research Department, Korea Institute of Science and Technology Information, P.O.Box 122, Yusong, Daejon 305-806, South Korea*

Abstract

We study the effect of external harmonic forcing on a one-dimensional complex Ginzburg–Landau equation (CGLE). For a sufficiently large forcing amplitude, a homogeneous state with no spatial structure is observed. As the forcing amplitude decreases, the state becomes unstable, forming a spatially periodic "stripe" state via a supercritical bifurcation. An approximate phase equation is derived, and an analytic solution for the stripe state is obtained. As the forcing amplitude decreases even further, the system undergoes a depinning transition into the state where the average phase has a non-zero velocity.
© 2002 Elsevier Science B.V. All rights reserved.

PACS: 5.45.Xt; 89.75.Kd; 47.20.Ky

Keywords: Complex Ginzburg–Landau equation; Synchronization; Resonant forcing; Pattern formation

1. Introduction

Nonequilibrium pattern formation is widely observed in many physical, chemical and biological systems. Significant progresses have been made in the field during the last few decades. For example, it has been found that nonequilibrium patterns can be grouped into a few universality classes [1–3]. In many cases, such a system is in constant interaction with its environment, and understanding the effect of extrinsic perturbation is of great theoretical and practical importance. In particular, it is interesting

* Corresponding author.
E-mail address: jysoo@hpcnet.ne.kr (J. Lee).

0378-4371/02/$ - see front matter © 2002 Elsevier Science B.V. All rights reserved.
PII: S0378-4371(02)01243-8

to study the deformation of an existing pattern or the formation of a new pattern under an external forcing. Our understanding in such a direction is far from complete.

Petrov et al. and later Lin et al. studied the light sensitive Belousov–Zhabotinsky (BZ) reaction in an oscillatory regime in the presence of a periodic modulation of the intensity of illumination [4,5]. They observed "entrainment bands" in which the system is frequency locked. Different spatial patterns—stationary fronts, standing waves of labyrinth and more complex shapes—are observed within the bands. In a similar BZ reaction setup, Vanag et al. studied spatial patterns and transitions among them in detail, and observed localized irregular/standing clusters as well as the above patterns [6,7].

Continuum models of forced pattern forming systems can be grouped into ones based on a kinetic model or on an amplitude equation. In the first group, an unforced system is modeled by a coupled kinetic model, such as the Brusselator, Oregonator or FitzHugh–Nagumo model, and parameters in the model are modulated to simulate the effect of external forcing (e.g. Refs. [5,8]). On the other hand, near a bifurcation onset of a pattern, small differences among systems become irrelevant, and they are all described by one of a few universal equations. If the bifurcation is supercritical and oscillatory, and if the most unstable wavenumber is zero, the complex Ginzburg–Landau equation (CGLE) is the equation for the class of systems. In the presence of an external periodic modulation, it is shown that the CGLE with an additional forcing term becomes the appropriate equation [3,9]. There exist a few studies on forced CGLE, and diverse behaviors are observed depending on several factors, such as the spatial dimension, the mode of the frequency locking, and the behavior of the corresponding unforced system [3,9–16]. However, we do not even know what behaviors are possible, let alone understand them.

Even the simplest case of the 1:1 locking in one dimension displays a wide variety of behaviors. At large amplitude of the forcing, a homogeneous state with no spatial structure is stable. Chaté et al. found that the homogeneous state becomes unstable to a periodic "stripe" or "kink-breeding" state as the forcing amplitude decreases, and "turbulent synchronized" state—chaotic with its average phase is locked to that of the forcing—can appear, as the amplitude decreases further [13].

In this paper, we study in detail the homogeneous and stripe states of one-dimensional forced CGLE around the 1:1 locking. There are two borders regarding the homogeneous state: (1) the stability border, below which the state loses its stability, and (2) the existence border, below which a homogeneous solution does not exist. In general, the existence and stability borders do not coincide. It is known that the stability border of the homogeneous state lacks a reflection symmetry around the $\nu = \alpha$ line. Here, ν is the difference between the natural and external frequency, and α is a non-linear detuning parameter. We find the asymmetry can be explained by the linear stability of the state. Also, the condition under which the existence and stability borders of the homogeneous state coincide is found. The stability border of the stripe state also lacks a reflection symmetry. An approximate phase equation is derived from the forced CGLE, and it is found that its qualitative behavior is identical to that of the original equation, at least in the region of present interest. An analytic expression of the stripe state for the phase equation is obtained, which is used to explain the asymmetry of the border of the stripe state.

As the forcing amplitude decreases even further, the average phase of the system starts to fluctuate, then acquires a non-zero average velocity, which is called "depinning". The quantitative behavior near the transition, for a certain range of parameters, can be described by an argument involving the type-I intermittency [17].

2. Forced complex Ginzburg–Landau equation

2.1. Complex Ginzburg–Landau equation

Near the stability border of a homogeneous state of an extended pattern forming system, the time evolution in a large spatial and temporal scale is given by one of a few universal equations [1–3]. If the instability is oscillatory and supercritical, and the wavenumber of the most unstable mode is zero, the complex Ginzburg–Landau equation (CGLE),

$$\partial_t A = A - (1 + i\alpha)|A|^2 A + (1 + i\beta)\nabla^2 A \tag{1}$$

is the governing equation. Here, A is complex amplitude, and α, β are real constants. The behavior of the CGLE is relatively well understood, especially in one and two dimensions [18–20]. It has plane wave solutions, which are stable only if $1 + \alpha\beta > 0$. Otherwise, the Benjamin–Feir instability sets in, making the solutions unstable. Near the unstable side of the stability border ($1 + \alpha\beta = 0$ line), "phase turbulence" is observed, which is characterized by disordered cellular structure and the absence of a defect ($|A| = 0$). "Defect turbulence" is observed further in the unstable region, where constant creation and annihilation of defects is observed [21,22]. In this paper, the value of $\alpha = -\frac{3}{4}$, $\beta = 2$ is mainly used, which is in the phase turbulence region.

2.2. Homogeneous state

Consider the case that a sinusoidal forcing is applied to the system of Eq. (1). It was shown that an additional forcing term should be included, and its form can be determined from the conditions of the spatial and temporal translation invariance [9]. For a harmonic forcing (near the 1:1 tongue), the resulting equation is

$$\partial_t A = (1 + iv)A - (1 + i\alpha)|A|^2 A + (1 + i\beta)\nabla^2 A + B\,, \tag{2}$$

where v is the difference between the natural and forcing frequency, and B is related to the amplitude of the forcing.

We first seek for the homogeneous solution of Eq. (2). In polar coordinates ($A = R\exp(i\Phi)$), the equation becomes

$$\begin{aligned} \partial_t R &= R - R^3 + B\cos\Phi + R_{xx} - \beta R\Phi_{xx} - 2\beta R_x\Phi_x - R\Phi_x^2\,, \\ R\partial_t\Phi &= vR - \alpha R^3 - B\sin\Phi + \beta R_{xx} + R\Phi_{xx} + 2R_x\Phi_x - \beta R\Phi_x^2\,. \end{aligned} \tag{3}$$

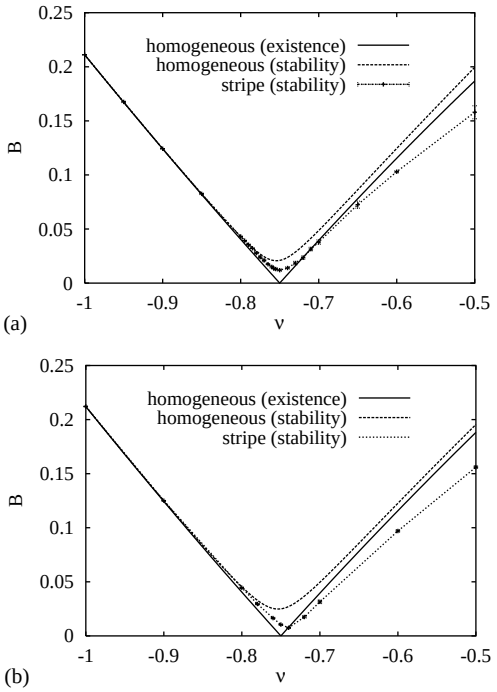

Fig. 1. (a) The existence and stability borders of the homogeneous state for the harmonically forced CGLE Eq. (2) with $\alpha = -\frac{3}{4}$ and $\beta = 2$. The stability border of the stripe state is also shown. Note that the stability borders are not symmetric to the $\nu = \alpha$ line. (b) Corresponding borders for the phase equation Eq. (9) with $\alpha = -\frac{3}{4}$, $\beta = 2$, and $R_0 = 1$.

For a sufficiently large B, the system is expected to lock to the forcing. Its homogeneous solution is

$$B\cos\Phi_0 = -R_0(1 - R_0^2)\,,$$

$$B\sin\Phi_0 = R_0(\nu - \alpha R_0^2)\,, \tag{4}$$

which can have 1 or 3 roots depending on the parameters. For the 3 roots case, only the one corresponding to the largest R_0 is stable. The region of the parameter space in which a locked homogeneous solution exists is shown in Fig. 1(a).

We apply the linear stability analysis to the homogeneous solution [13], where the behavior of a small deviation from the solution $r = R - R_0$ and $\phi = \Phi - \Phi_0$ is studied. The growth rate of the mode with wavenumber k is found to be

$$\lambda(k) = 1 - 2R_0^2 - k^2 + \sqrt{(1+\alpha^2)R_0^4 - (\nu - 2\alpha R_0^2 - \beta k^2)^2}\,, \tag{5}$$

which has the maximum value of

$$\lambda_{\max} = 1 - 2R_0^2 - \frac{1}{\beta}\left[v - (2\alpha + \sqrt{(1+\alpha^2)(1+\beta^2)})R_0^2\right] \tag{6}$$

at $k = k_{\max}$, corresponding to the most unstable mode, which is given by

$$\beta k_{\max}^2 = v - \left(2\alpha + \sqrt{\frac{1+\alpha^2}{1+\beta^2}}\right) R_0^2 \,. \tag{7}$$

The stability border B_s of the homogeneous solution is obtained by solving numerically $\lambda_{\max} = 0$, which is also shown in Fig. 1(a).

A distinct feature of the stability border is that it is not symmetric to the $v = \alpha$ line. As shown in the figure, the difference between the existence and stability border is smaller at the $v < \alpha$ side. Moreover, the difference vanishes for $v \leqslant v_c$ with $v_c \simeq -1.067$. This feature can be understood from the v dependence of $k_{\max}$, which is given by Eq. (7). It is found that $k_{\max}$ is an increasing function of v: it is zero for $v \leqslant v_c = (2\alpha + \sqrt{(1+\alpha^2)/(1+\beta)})R_0^2$, and proportional to $\sqrt{v - v_c}$ slightly above v_c. Since the wavenumber of the most unstable mode is zero for $v \leqslant v_c$, and since the solution Eq. (4) with the largest R_0 is stable to a zero wavenumber perturbation, the existence of the homogeneous solution guarantees its stability.

As will be discussed later, an approximate phase equation is derived from Eq. (2), which gives an additional insight on the stability border. The origin of the instability of the homogeneous state of the phase equation can be traced to a Laplacian term, whose coefficient is a decreasing function of v, and becomes negative at v_c^{ϕ}. Thus, the homogeneous state is stable for $v \leqslant v_c^{\phi}$, and it becomes more unstable as v increases.

2.3. Stripe state

The behavior below the stability border is investigated numerically. The forced CGLE in one dimension is integrated using a pseudo-spectral method for various v and B [23]. The spatial resolution Δx and timestep Δt used is 0.1 and 0.01, respectively. Also, a periodic boundary condition is used. For most cases, the linear size of the system is chosen to be 4096, and the time interval of 2×10^4 is used. Larger systems for longer intervals are also studied, and no change in the behavior is observed.

The numerical integrations confirm the prediction that the homogeneous state is stable above the stability border. It is found that the state undergoes a supercritical bifurcation to a spatially periodic static "stripe" state as B decreases below the border, and the modulation amplitude of the state, defined as $\delta\phi = \sqrt{\langle(\phi - \langle\phi\rangle_x)^2\rangle_x}$, behaves as $\sqrt{B_s - B}$ close to the border (Fig. 2(a)). The wavenumber of the stripe state is found to agree very well with $k_{\max}$ of Eq. (7), especially near the border. In order to check how the nature of the transition depends on the unforced dynamics, the transition from a homogeneous state is examined for four different values of (α, β): $(-2, 2)$, $(-1.11, 1)$, $(-2, 0)$ and $(-0.75, 0.5)$. It is found that a supercritical transition to the stripe state is observed for the first two cases belonging to the Benjamin–Feir (BF) unstable region,

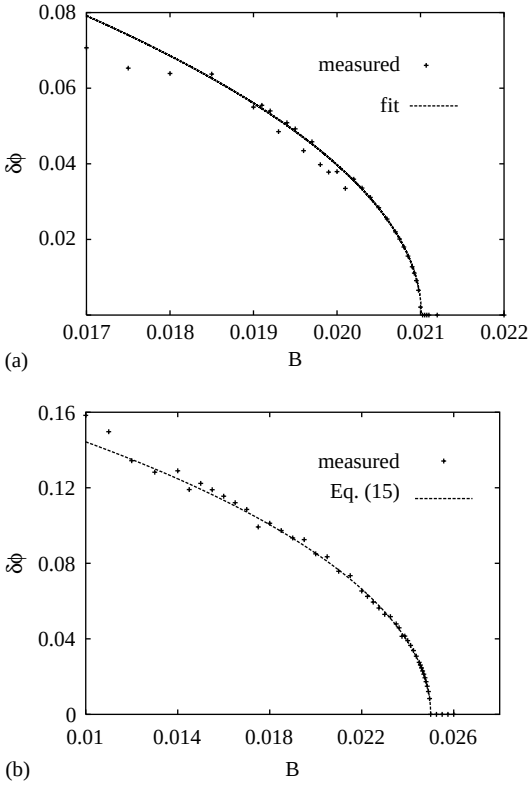

Fig. 2. (a) The modulation amplitude $\delta\phi$ of the stripe solution of the forced CGLE Eq. (2) is shown against B for $v=-0.75$. Also shown is a square root fit $D\sqrt{B_s-B}$ with $D=1.25$ and $B_s=0.02101$. (b) $\delta\phi$ of the stripe solution of the phase equation Eq. (9) is shown for $v=-0.75$. Analytic expression Eq. (15) with the coefficients given by Eq. (17) is found to be a good approximation.

while a transition to a disordered structure is observed for the other two cases belonging to the BF stable region.

As B decreases further, the stripe state becomes unstable to a fluctuating stripe or "kink-breeding" state, depending on v [13]. The stability border of the stripe state is determined, and plotted in Fig. 1(a). Again, the border is not symmetric to the $v=\alpha$ line. The region of the stripe state is much broader on the $v>\alpha$ side. Moreover, it extends to the region where a locked homogeneous state does not exist. The origin of the asymmetry will be discussed using a phase equation, and is found to be very different from the case of the homogeneous state.

2.4. Depinning transition

As B decreases below the stability border of the stripe solution, the average phase of the system starts to fluctuate in time. As B decreases even further, the time-averaged velocity of the average phase $\Omega\equiv\lim_{T\to\infty}(1/T)\langle\phi(x,T)-\phi(x,0)\rangle_x$ becomes non-zero,

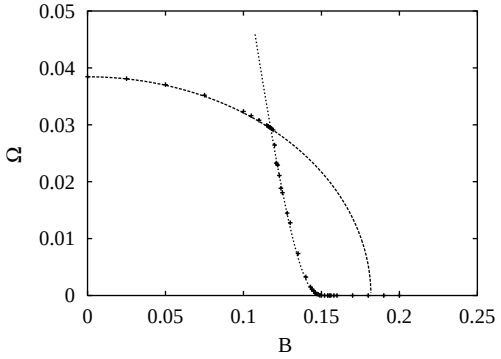

Fig. 3. The velocity of the average phase Ω is plotted against B for $v=-0.5$. The dashed line shows square root fitting $E\sqrt{B_1-B}$ with $E=0.0384$ and $B_1=0.1817$ for small B. The dotted line shows the type-I intermittency based expression—$F\exp(-G/\sqrt{B_c-B})$ with $F=1.55$, $G=0.7651$ and $B_c=0.1547$.

which will be termed as "depinning" transition. Depending on the value of v, there are a few possibilities of depinning. One is "depinning due to kink-breeding", where the average velocity is determined by the properties of the kink, such as its nucleation rate and average velocity. Around $v=\alpha$, the kink-breeding is no longer present, and depinning occurs when a part of the system fluctuates and its phase advances (or jumps) by an amount close to 2π, and other part of the system follows it. In this regime, the average velocity will be determined by the "jump" rate. We find that the average velocity Ω near the transition is well described by the expression based on the type-I intermittency—$\exp(-G/\sqrt{B_c-B})$ [17] (Fig. 3). For very small value of B, the phase does not advance by jumps, but by smooth and constant increases. In this regime, Ω is well fitted by a "mean field" result of $\sqrt{B_1-B}$, which is also plotted in Fig. 3.

3. Phase equation

3.1. Derivation

An approximate phase equation can be derived from Eq. (2) as follows. Define small variables $r=R-R_0$ and $\phi=\Phi-\Phi_0$, and assume that the time scale for ϕ is much larger than that for r. The variable r is then slaved to ϕ. Starting from Eq. (3), it can be shown

$$r=\frac{R_0}{3R_0^2-1}\left[(1-R_0^2)+\frac{B}{R_0}\cos(\Phi_0+\phi)-\beta\phi_{xx}-\phi_x^2\right], \tag{8}$$

where additional terms higher than the second order in ϕ are ignored, and B is assumed to be small. Substituting this to the phase part of Eq. (3),

$$R_0\partial_t\phi=vR_0-\alpha R_0^3-B\sqrt{1+a^2}\sin(\Phi_0+\phi+\delta)+b\phi_x^2+c\phi_{xx}+d\phi_{xxxx}+e\,, \tag{9}$$

where a, b, c, d, e, δ are constants depending on α, β, ν and R_0. Since R_0 is 1 at $\nu = \alpha$, and is a slowly varying function of ν, it is expected that setting $R_0 = 1$ does not change the qualitative behavior of the equation. On the other hand, the constants are simplified to

$$a = \alpha - (\nu - \alpha)/2\,,$$

$$b = \alpha - \beta - (\nu - \alpha)/2\,,$$

$$c = 1 + \alpha\beta - \beta(\nu - \alpha)/2\,,$$

$$d = -\beta^2/2\,,$$

$$e = 0\,,$$

$$\delta = \tan^{-1}(a)\,. \tag{10}$$

For the remainder of the paper, R_0 will be set to 1 in the equation. Note that Eq. (9) is a generalized version of the phase equation obtained by Coullet and Emilsson, which is derived for the special case of $\nu \simeq \alpha$ [9]. Also, ϕ_{xxxx} term is added for the stability of the solution in the phase and defect turbulence regions.

3.2. Homogeneous state

The phase equation is studied in a way parallel to the analysis of the forced CGLE. Homogeneous states, given by

$$\Phi_0 = \sin^{-1}\left(\frac{\nu - \alpha}{B\sqrt{1 + a^2}}\right) - \delta \tag{11}$$

exist for $B \geqslant (\nu - \alpha)/\sqrt{1 + a^2}$. There exist two solutions, Φ_0^{s} and Φ_0^{u}, in the $[0, 2\pi]$ interval satisfying Eq. (11) as shown in Fig. 4. The Φ_0^{s} solution is stable under homogeneous perturbation, while the Φ_0^{u} solution is unstable. A linear stability analysis of the stable homogeneous state shows that the maximum growth rate is

$$\lambda_{\max}^{\phi} = -B\sqrt{1 + a^2}\cos(\Phi_0 + \delta) - c^2/4d \tag{12}$$

for the mode with wavenumber $k_{\max}^{\phi} = \sqrt{c/2d}$ (if $c \leqslant 0$). The state is found to be linearly stable above the stability border B_{s}^{ϕ}, which is given as

$$B_{\mathrm{s}}^{\phi} = \sqrt{\frac{(c^2/4d)^2 + (\nu - \alpha)^2}{1 + a^2}}\,. \tag{13}$$

The existence and stability borders are plotted in Fig. 1(b) for $\alpha = -\frac{3}{4}$, $\beta = 2$. Note that the shape of the borders are qualitatively the same as those of the forced CGLE: the

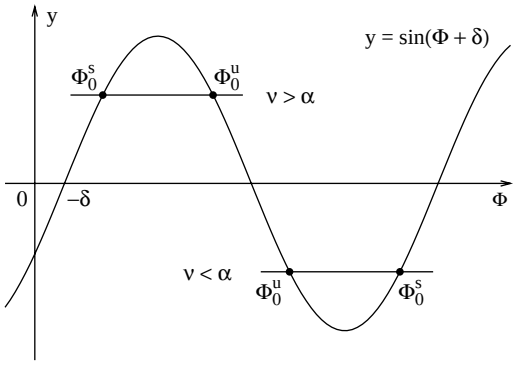

Fig. 4. A schematic view for the determination of the homogeneous solution of the phase equation Eq. (9): There exist one stable Φ_0^s and one unstable Φ_0^u solutions. Here, the one with positive $\cos(\Phi_0 + \delta)$ is stable. For $\nu > \alpha, \Phi_0^u > \Phi_0^s$, while $\Phi_0^u < \Phi_0^s$ for $\nu < \alpha$.

stability border is asymmetric to the $\nu = \alpha$ line, and the two borders meet for $\nu \leqslant \nu_c^\phi$. Since the wavenumber of the most unstable mode should be zero at $\nu = \nu_c^\phi$, one arrives at

$$\nu_c^\phi = \frac{2 + 3\alpha\beta}{\beta} . \tag{14}$$

For the above values of α and β, $\nu_c^\phi = -\frac{5}{4}$, which is comparable to the value of ν_c for the forced CGLE.

The simple structure of the phase equation makes its interpretation simple. The reason for the instability is that c can be negative, while the ϕ_{xxxx} term always tries to suppress such an instability. The value of c remains positive for $\nu < \nu_c^\phi$, and the homogeneous state is stable. As ν increases further, c becomes negative. Since c is a decreasing function of ν, the instability becomes stronger with increasing ν, which explains the fact that the difference between the existence and stability border increases with ν.

3.3. Stripe state

The behavior of the phase equation below the stability border is studied numerically. As one crosses the border, the homogeneous state goes through a supercritical bifurcation to a stripe state, and the modulation amplitude $\delta\phi = \sqrt{\langle(\phi - \langle\phi\rangle_x)^2\rangle_x}$ behaves as $\sqrt{B_s^\phi - B}$ close to the border. A typical dependence of $\delta\phi$ on B is shown in Fig. 2(b), where $\nu = -0.75$. As B decreases further, the stripe state becomes unstable. The stability border of the stripe state determined numerically is plotted in Fig. 1(b). Again, the border is not symmetric to the $\nu = \alpha$ line, and even extends below the existence border of the homogeneous state. Although the phase equation is simpler

than the forced CGLE, their qualitative behaviors are essentially the same, at least for the homogeneous and stripe states.

The simple structure of the phase equation allows an analytic expression for the stripe solution. The solution may be expanded in terms of harmonic functions

$$\phi(x) = \phi_1 + S_1 \sin k_0 x + C_1 \cos k_0 x + S_2 \sin 2k_0 x + C_2 \cos 2k_0 x \,, \tag{15}$$

where higher harmonics are ignored. k_0 is the wavenumber of the most unstable mode, and the coefficient C_1 can always be set to 0 by choosing an appropriate origin. Substituting it to Eq. (9), we find

$$\begin{aligned}
&S_2 = 0 \,, \\
&\sin(\Phi_0 + \phi_1 + \delta) = \frac{v - \alpha + (S_1^2 + 4C_2^2)bc/4d}{B\sqrt{1+a^2}(1 - (S_1^2 + C_2^2)/4)} \,, \\
&S_1^2 = 4C_2 \, \frac{-B\sqrt{1+a^2}\cos(\Phi_0 + \phi_1 + \delta) + 2c^2/d}{B\sqrt{1+a^2}\sin(\Phi_0 + \phi_1 + \delta) - bc/d} \,, \\
&C_2 = 2 \, \frac{-B\sqrt{1+a^2}\cos(\Phi_0 + \phi_1 + \delta) - c^2/4d}{B\sqrt{1+a^2}\sin(\Phi_0 + \phi_1 + \delta) + 2bc/d} \,,
\end{aligned} \tag{16}$$

which can be solved numerically for S_1, C_2 and ϕ_1. Near the stability border B_s^{ϕ}, an approximate analytic solution can be obtained, which is

$$\begin{aligned}
&S_1 \propto \sqrt{B_s^{\phi} - B} \,, \\
&C_2 \propto S_1^2 \,, \\
&\phi_1 \simeq \frac{1}{4B\sqrt{1+a^2}\cos(\Phi_0 + \delta)} \left(v - \alpha + \frac{bc}{d} \right) S_1^2 \,,
\end{aligned} \tag{17}$$

where the proportionality constants are rather complex except for the case of ϕ_1. The analytic solution agrees well with the results using numerical integration: as shown in Fig. 2(b), the modulation amplitude $\delta\phi$ vs. B curve obtained from the above expression is in good agreement with the corresponding numerical values.

Not only the analytic solution confirms the square root dependence of A_1, it also provides an explanation for the asymmetry of the stability border of the stripe solution. There are two homogeneous solutions—stable Φ_0^s and unstable Φ_0^u—of the phase equation with B a little below the stability border. As B decreases from the homogeneous toward the stripe region, the modulation amplitude around Φ_0^s increases with decreasing B. For sufficiently small B, $\phi(x)$ at certain x approaches the unstable fixed point Φ_0^u, which then makes the stripe solution unstable. Note that ϕ_1 in Eq. (17) is non-zero—it is negative when v is not very different from α. Thus, the average phase of a stripe state is shifted toward a value smaller than Φ_0^s. The average phase of the stripe solution measured using numerical integration is also confirms the shift. As shown in

Fig. 4, the shift moves the stripe solution toward (away from) Φ_0^u for $v < \alpha$ ($v > \alpha$), resulting in the asymmetry (a related argument is given in Ref. [15]). The situation is entirely similar for the forced CGLE: the average phase is shifted toward (away from) the unstable solution for $v < \alpha$ ($v > \alpha$).

4. Conclusion

Despite its simplicity, the forced CGLE displays a large variety of phenomena. The homogeneous and stripe states are mainly discussed here, and the phase equation is found to be very useful in understanding the stability borders of the forced CGLE. For a sufficiently large forcing amplitude, a homogeneous state with no spatial structure is observed. The state becomes unstable to a spatially periodic stripe state via a supercritical bifurcation as the forcing amplitude decreases. We obtained an analytic solution for the stripe state of the phase equation, through which an argument for the asymmetry of the stability border of the state is formulated. As B decreases further, the system undergoes a depinning transition into the state where the average phase has a non-zero velocity. We found a few types of depinning, including "depinning by kink-breeding" or one based on the type-I intermittency.

Acknowledgements

This work was supported in part by Grant No. 2000-2-11200-002-3 from the BRP program of the KOSEF. J. Lee is supported in part by Creative Research Initiatives of the Korean Ministry of Science and Technology.

References

[1] M.C. Cross, P.C. Hohenberg, Rev. Mod. Phys. 65 (1993) 851.
[2] P. Manneville, Dissipative Structures and Weak Turbulence, Academic Press, New York, 1990.
[3] D. Walgraef, Spatio-Temporal Pattern Formation, Springer, New York, 1997.
[4] V. Petrov, Q. Ouyang, H.L. Swinney, Nature (London) 388 (1997) 655.
[5] A.L. Lin, M. Bertram, K. Martinez, H.L. Swinney, A. Ardelea, G.F. Carey, Phys. Rev. Lett. 84 (2000) 4240.
[6] V.K. Vanag, L. Yang, M. Dolnik, A.M. Zhabotinsky, I.R. Epstein, Nature (London) 406 (2000) 389.
[7] V.K. Vanag, A.M. Zhabotinsky, I.R. Epstein, Phys. Rev. Lett. 86 (2001) 552.
[8] O. Steinbock, V. Zykov, S.C. Müller, Nature (London) 366 (1993) 322.
[9] P. Coullet, K. Emilsson, Physica D 61 (1992) 119.
[10] P. Coullet, J. Lega, B. Houchmanzadeh, J. Lajzerowicz, Phys. Rev. Lett. 65 (1990) 1352.
[11] C. Elphick, A. Hagberg, E. Meron, Phys. Rev. Lett. 80 (1998) 5007.
[12] C. Elphick, A. Hagberg, E. Meron, Phys. Rev. E 59 (1999) 5285.
[13] H. Chaté, A, Pikovsky, O. Rudzick, Physica D 131 (1999) 17.
[14] A.L. Lin, A. Hagberg, A. Ardelea, M. Bertram, H.L. Swinney, E. Meron, Phys. Rev. E 62 (2000) 3790.
[15] H.-K. Park, Phys. Rev. Lett. 86 (2001) 1130.
[16] R. Gallego, D. Walgraef, M. San Miguel, R. Toral, nlin/0104059, preprint.
[17] A. Pikovsky, G. Osipov, M. Rosenblum, M. Zaks, J. Kurths, Phys. Rev. Lett. 79 (1997) 47.

[18] B.I. Shraiman, A. Pumir, W. van Saarloss, P.C. Hohenberg, H. Chaté, M. Holen, Physica D 57 (1992) 241.
[19] H. Chaté, Nonlinearity 7 (1994) 185.
[20] H. Chaté, P. Manneville, Physica A 224 (1996) 348.
[21] P. Coullet, J. Lega, Europhys. Lett. 7 (1988) 511.
[22] P. Coullet, L. Gil, J. Lega, Phys. Rev. Lett. 62 (1989) 1619.
[23] C.A.J. Fletcher, Computational Techniques for Fluid Dynamics, Springer, New York, 1991.